

## A Monte Carlo study of the BNNNI model

This article has been downloaded from IOPscience. Please scroll down to see the full text article.

1989 J. Phys. A: Math. Gen. 22 3981

(<http://iopscience.iop.org/0305-4470/22/18/031>)

View [the table of contents for this issue](#), or go to the [journal homepage](#) for more

Download details:

IP Address: 129.252.86.83

The article was downloaded on 01/06/2010 at 07:00

Please note that [terms and conditions apply](#).

## A Monte Carlo study of the BNNNI model

M Aydın† and M C Yalabık

Physics Department, Bilkent University, Ankara, Turkey

Received 30 September 1988, in final form 22 May 1989

**Abstract.** The biaxially next-nearest-neighbour Ising (BNNNI) model is studied using the Monte Carlo procedure. The structure factor is used to identify the possible phases of the system. At intermediate temperatures, evidence for the presence of an additional incommensurate phase with a varying wavevector between the disordered and antiphase states is given.

### 1. Introduction

The biaxially next-nearest-neighbour Ising (BNNNI) model can be defined by the two-dimensional Hamiltonian:

$$\frac{-H}{kT} = K_1 \sum_{\langle i,j \rangle} s_i s_j + K_2 \sum_{\langle\langle i,j \rangle\rangle} s_i s_j \quad (1)$$

where the first summation is over all nearest-neighbour pairs and the second summation is over all axially next-nearest-neighbour pairs of Ising spins  $s_i$  (with  $s_i = \pm 1$ ).  $K_1$  and  $K_2$  are the nearest and axially next-nearest couplings, respectively ( $K = J/kT$  with  $J$  the magnetic interaction between neighbouring spins,  $k$  the Boltzmann constant and  $T$  the temperature).

Early studies on the model were done by Hornreich *et al* (1979), Selke and Fisher (1980) and Selke (1981). Later the model was analysed by the series analysis method (Oitmaa and Velgakis 1987), finite lattice methods (Oitmaa *et al* 1987) and Monte Carlo methods (Landau and Binder 1985, Velgakis and Oitmaa 1988).

The model has one disordered (paramagnetic) and at least three ordered states (a ferromagnetic state, an antiphase state, in which the four spins in a two by two unit cell alternate in direction in neighbouring cells, and an antiferromagnetic state). In the work by Landau and Binder it was found that there is a single transition between disordered and antiphase states. In other works, no clear evidence is given about the type of the transition between these states.

In the recent work by Aydın and Yalabık (1989), the phase diagram of the BNNNI model has been obtained using the renormalisation group (RG) method. It is observed that there is a single transition between disordered and antiphase states at high temperatures and that there is evidence for an additional new phase between these phases at intermediate and low temperatures. The main features of this phase could not be determined since its ground state is not conserved by the RG transformation used in this study.

In the present work, the BNNNI model is studied using the Monte Carlo method. Evidence is presented for the existence of an incommensurately ordered phase (whose

† Present address: School of Physics, The University of New South Wales, Kensington, NSW 2033, Australia.

presence in the  $BNNNI$  model was conjectured earlier by Aydın and Yalabık, (1989) as well as the regular antiphase, ferromagnetic and antiferromagnetic phases.

The next section gives a description of the method used for the simulation and analysis. The results are summarised in the last section.

## 2. Method and analysis

In the present work, the  $BNNNI$  model is studied using the Monte Carlo method. Starting from a random initial configuration or from an ordered ground state, the system is relaxed using the standard Monte Carlo procedure (Binder and Stauffer 1984). Time is measured in Monte Carlo steps (MCS). When the number of flipped spins is equal to the total number of spins (not necessarily each spin of the system is flipped), the system is said to relax for one MCS. Computations are carried out up to 10 000 MCS on a  $128 \times 128$  lattice. The structure factor, time variations of energy, nearest-, next-nearest, axially next-nearest-neighbour correlations and the magnetisation are obtained for various sets of  $K_1$  and  $K_2$  values. The resulting phase diagram is given in figure 1. When  $K_1 = 0$ , the system decomposes into four independent two-dimensional Ising lattices with nearest-neighbour coupling  $K_2$ . The exact value for the critical coupling is  $K_c = 0.44\dots$ , which is shown in the phase diagram (figure 1(a)) for this case and for the case  $K_2 = 0$  as well. (The latter case simply corresponds to the two-dimensional Ising model with a nearest-neighbour coupling  $K_1$ .)

The structure factor of the system is obtained using the relation

$$S(i, j) = \left( \frac{S_S(i, j)}{N_S} \right)^{1/2} \quad (2)$$

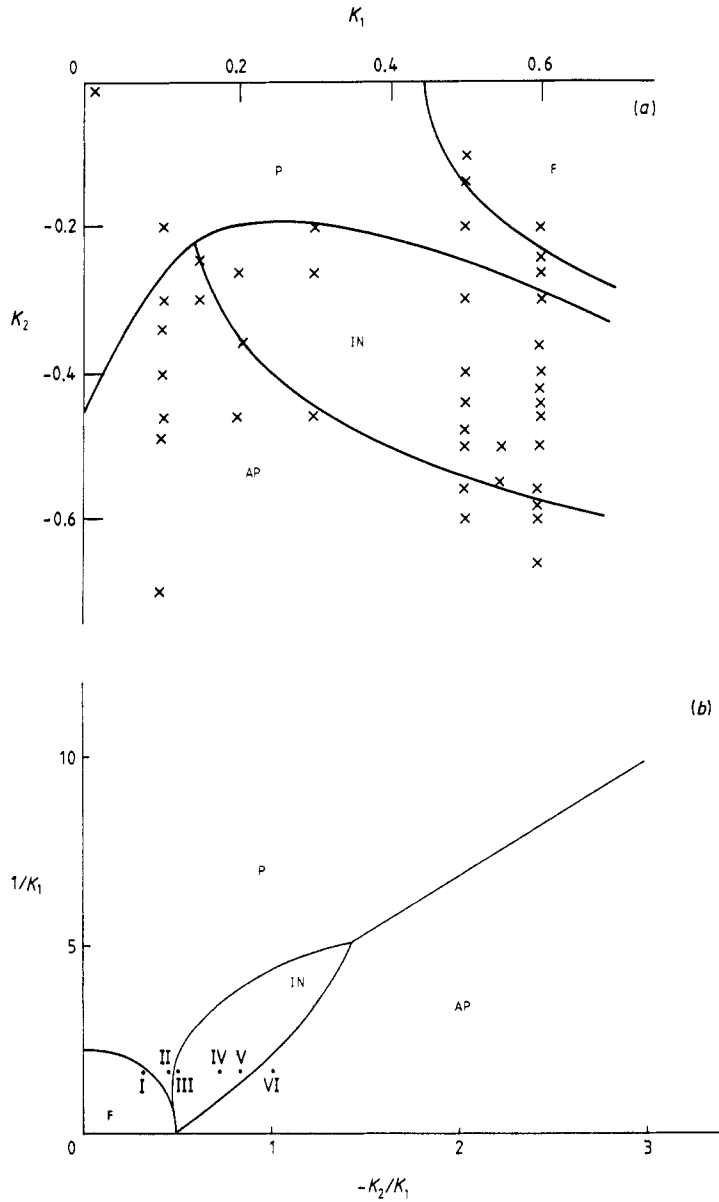
where  $S_S(i, j)$  is given by the formula

$$S_S(i, j) = \frac{1}{N^2} \sum_{t=\Delta t}^{N_S \Delta t} F_S(i, j; t). \quad (3)$$

Here  $N^2$  is the total number of spins in the system ( $N = 128$ ). The function  $F_S(i, j)$  is calculated at various time intervals such as 10, 20, 100, 200, 500,  $\dots$ , MCS for various sets of  $K_1$  and  $K_2$  and it is averaged over the values obtained at these intervals. The factor  $N_S$  in equation (2) is the number of evaluations of the function  $F_S(i, j)$ . The function  $F_S(i, j)$  is obtained by taking the Fourier transform of the two-dimensional autocorrelation function, using a fast Fourier algorithm. The three-dimensional plots of  $S(i, j)$  against  $i$  and  $j$  are obtained for various sets of  $K_1$  and  $K_2$  values. These plots show clearly the phase of the system, if it is one of the phases, namely ferromagnetic, antiferromagnetic and antiphase states. When  $S(i, j)$  is plotted along the (1, 1) direction (i.e. for  $i = j$ ), it is possible to identify all phases clearly. (The system is symmetric around the axis along the (1, 1) direction.) The point  $i = j = l_m$  where  $S(i, j)$  has a maximum gives the magnitude of the wavevector of the underlying phase. The components  $k_x = k_y = k_m$  of the corresponding wavevector can be calculated using the relation

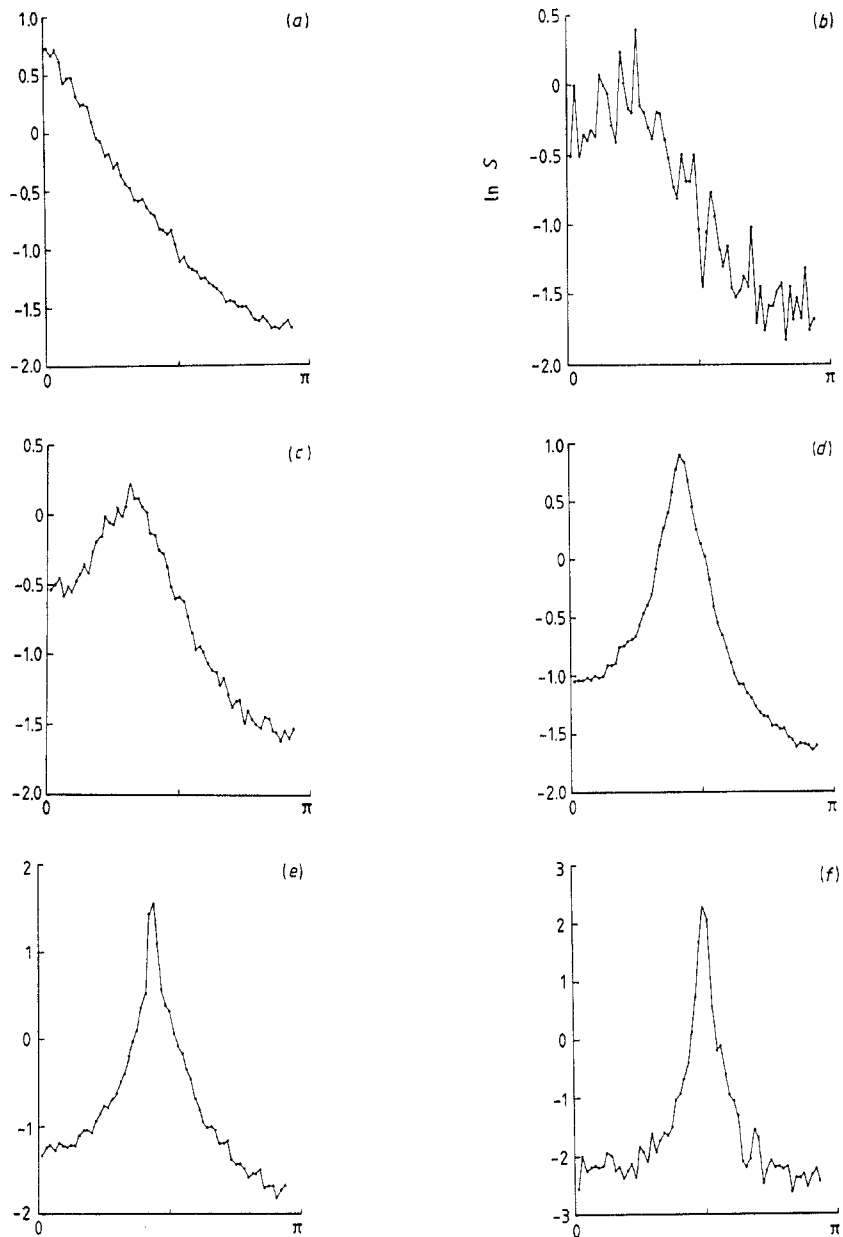
$$k_m = \frac{2\pi l_m}{N}. \quad (4)$$

Figure 2 displays the structure factor  $S(k_x, k_y)$  plotted along the (1, 1) direction as a function of  $k_x = k_y$  for certain values of the coupling constants. The structure factor



**Figure 1.** The phase diagram obtained as a result of this work. The points in (a) correspond to the coupling constant values used in the simulation. The points identified by I, II, etc, in (b) are referred to in figure 2. IN represents the incommensurate, F the ferromagnetic, P the paramagnetic, and AP the antiphase states. The phase separation lines were drawn roughly, based on the nature of the structure function at the simulation points.

is calculated by averaging  $S(i, j)$  over eight symmetric portions of the lattice as well. Two-dimensional plots, in the form of contours showing equal structure factor values, are obtained for each set of  $K_1$  and  $K_2$  values at which Monte Carlo simulation is carried out. Although two different type of plots give the same results, the value of  $k_m$  can be obtained more easily and more precisely using  $S(k_x = k_y)$  plots. In figure



**Figure 2.** Plots of the logarithm of the structure function along the (1, 1) direction, for the coupling constant values shown in figure 1. The value of  $k_x = k_y = k_m$  is shown on the abscissa.

2(a), the structure factor has a maximum at  $k_x = k_y = 0$ . This indicates that this set of  $K_1$  and  $K_2$  values ( $K_1 = 0.60$ ,  $K_2 = -0.20$ ) corresponds to a point which is in the ferromagnetic phase of the phase diagram given in figure 1(a). For some values of  $K_1$  and  $K_2$ , no distinctive peaks are noticeable in the structure function. It displays a random behaviour. Figure 2(b) is a typical plot of this kind which characterises the disordered phase. In figures 2(c)-(f),  $k_m$  varies between  $\pi/3$  and  $\pi/2$ . The structure

factor has a maximum at  $k_m = \pi/2$  in figure 2(f) ( $K_1 = 0.60, K_2 = 0.66$ ). This is an indication of the antiphase state.

In the phase diagram (figures 1(a), 1(b)), the region shown by 1N corresponds to a special type of phase in which  $k_m$  varies as  $K_2$  is varied for a fixed value of  $K_1$ . It occurs at a lower value than  $k_m = \pi/2$  when  $K_2$  is increased (for a fixed value of  $K_1$ ) starting from the boundary of the antiphase state. The variation of a wavevector is an indication of an incommensurate phase between disordered and antiphase states.

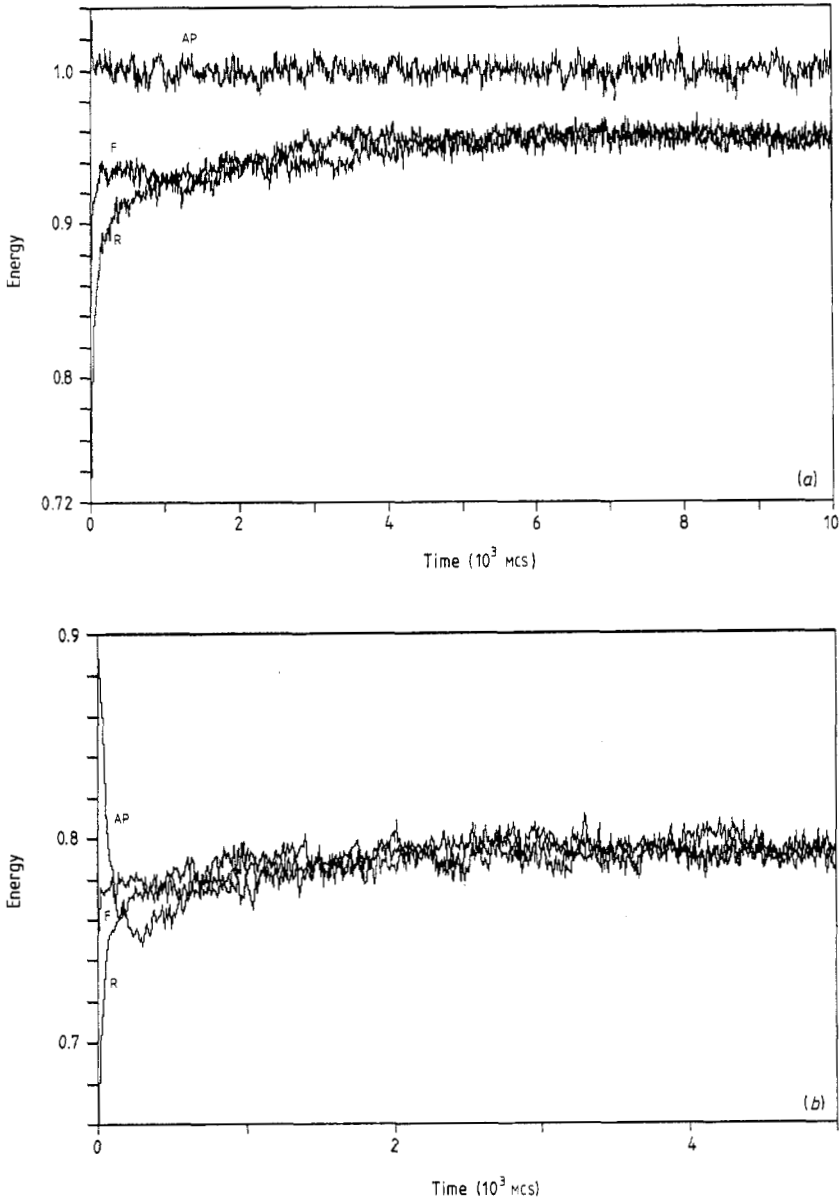


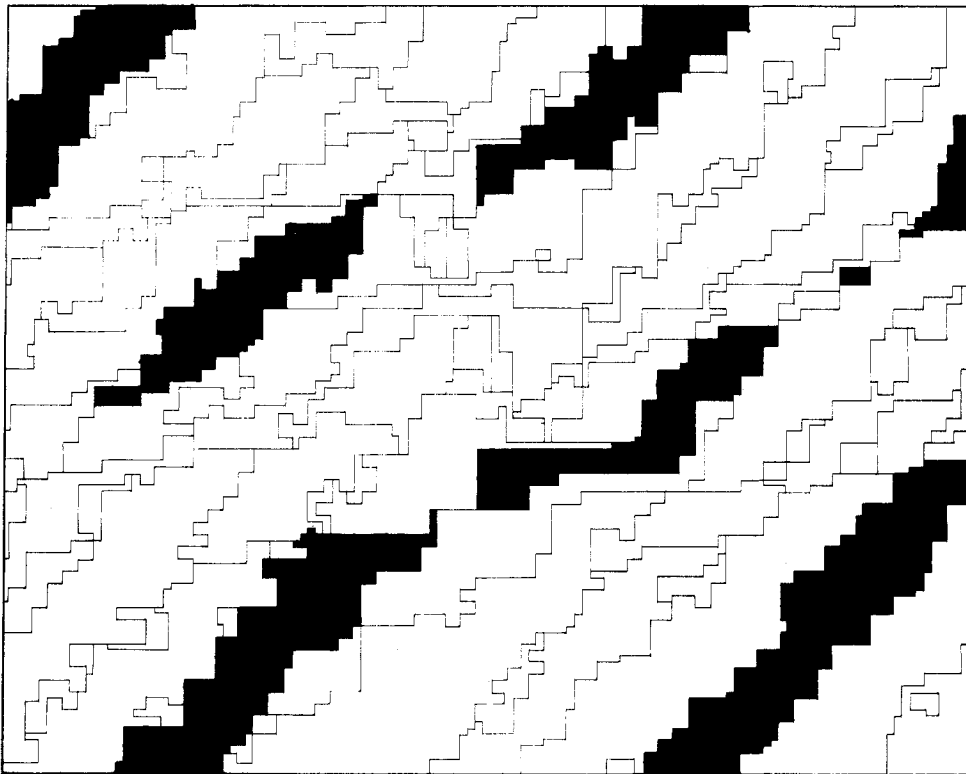
**Figure 3.** Relaxation of the system energy as a function of time for two points in the 1N phase. The letters next to the plots represent different types of starting configurations (R represents a random configuration). (a)  $K_1 = 0.55, K_2 = -0.55$ . (b)  $K_1 = 0.55, K_2 = -0.50$ .



state. Figure 3(a) shows the time variation of energy at a point ( $K_1 = 0.55$ ,  $K_2 = -0.55$ ) near the boundary between region IN and the antiphase state. It is obvious from this figure that one can reach equilibrium by starting either from a random configuration or from the ferromagnetic ground state. The time variation for a point in region IN is given in figure 3(b). For this particular set of values ( $K_1 = 0.55$ ,  $K_2 = -0.50$ ), equilibrium can be reached by starting from the antiphase ground state as well.

Figure 4(a) shows a lattice configuration for the set of values  $K_1 = 0.55$ ,  $K_2 = -0.55$ . Each letter denotes one of the sixteen degenerate ground states of the antiphase state. In figure 4(b), the presence of one particular ground state is indicated by the shaded regions. Unlike the other ordered phases, the boundaries between these ground states have a tendency to lie along the (1, 1) direction. The same character is observed when the procedure is repeated with different random initial configurations. The main shapes and features, such as the periods of repetition corresponding to domains of different ground states (whose corresponding peaks could be identified on the structure function), do not seem to change as the number of MCS is increased. This is further evidence for the appearance of the incommensurate phase in region IN of the phase diagram.

By repeating this procedure for a large number of coupling constant values (e.g. with small increments in  $K_2$  for fixed values of  $K_1$ ), a detailed phase diagram can be obtained. The types of transitions can be deduced by analysing the variations of



(b)

Figure 4. (continued)



correlation functions across these transitions. It is also necessary to see to what value  $k_m$  approaches at points near the disordered-antiphase phase boundary. A larger number of MCS would probably be required near the critical points due to the slowing down effects.

### 3. Results

In the present work, the  $BNNI$  model is analysed at various values of its coupling constants using the Monte Carlo simulation on a  $128 \times 128$  lattice. The time variations of energy, nearest-, next-nearest-, axially-next-nearest-neighbour correlations and the magnetisation are obtained. The time variation of energy is used to check the equilibrium conditions.

The structure function values are obtained using Fourier transforms of the spin variables of the system (equation (2)) and plotted along the (1, 1) direction. Some typical plots are shown in figure 2. These plots are used to identify the type of undergoing phase and to find the magnitude of the wavevector of that phase. The components  $k_x, k_y$  ( $k_x = k_y$ ) of the wavevector corresponds to the  $k_m$  value along the horizontal axis at which the structure function has a maximum. The antiphase state is characterised by a wavevector with components  $k_x = k_y = k_m = \pi/2$  along the (1, 1) direction. Starting from the boundary of the antiphase state,  $k_m$  has lower values as  $K_2$  is increased. For some values of  $K_2$ ,  $S(k_x, k_y)$  does not have a single distinctive peak, but a randomly varying character and it can be recognised as the disordered phase. The only phase appearing after this phase (when  $K_2$  is increased) is the ferromagnetic phase which has a single peak at  $k_x = k_y = k_m = 0$ .

The phase diagram is drawn roughly through the data points at which the Monte Carlo calculations are carried out. The structure factor data show that the phases with constant  $k_m$  value are the ferromagnetic, antiferromagnetic and antiphase states (with  $k_m = 0$ ,  $k_m = \pi$  and  $k_m = \pi/2$ , respectively). The variation of the wavevector between disordered and antiphase states at intermediate temperatures is an indication of an incommensurate phase between these phases. No peak other than the one with  $k_m = \pi/2$  is observed at high temperatures (for  $K_1 < 0.15$ ), when  $K_2$  is varied for a fixed value of  $K_1$ . This is the evidence of a single transition between antiphase and disordered states at these temperatures.

The main result of this work is the evidence presented for the existence of a phase with a varying wavevector at intermediate temperatures. The resulting phase diagram is not a detailed phase diagram obtained at sufficiently large numbers of data points. It only shows the main shape of the phase diagram and possible phases of the system. The structure factor is the quantity used to identify the possible phases of the system and to find the magnitudes of their corresponding wavevectors as well. The main character of the incommensurate phase can be observed by looking at spin values of the system which is sufficiently far away from equilibrium (figure 4). Degenerate ground states of this phase seem to have boundaries lying along the (1, 1) direction of the system.

Equilibrium can be reached in all regions of the phase diagram using a random initial configuration or ground state of an ordered state. 10 000 MCS seem sufficiently large to study the equilibrium behaviour of the system. The Monte Carlo method is expected to give better results as the lattice size is increased. However, this size ( $128 \times 128$ ) seems to be sufficiently large to obtain the phase diagram accurately. The

finite-size effects, which are not considered in this study, would be an interesting problem to explore using this method.

The statistical errors in this study are very small since large numbers of MCS are carried out for each data point in the phase diagram. (They are very small compared to the size of the data points.) The errors arise due to the lack of a sufficient number of data values (i.e. they depend on the increment of  $K_2$  values for a fixed value of  $K_1$  and also on the increment of  $K_1$ ). The same reason holds for our not being able to give the value of  $k_m$  at points near the incommensurate-disordered phase boundary and for not being able to give any specific information about the type of transition.

By repeating this procedure for large numbers of  $K_1$  values, with much smaller increments in  $K_2$  values, the type of transition along the disordered-antiphase state phase boundary can be found from the energy against  $K_2$  variation. It can also provide the magnitude of the wavevector in the incommensurate phase near the disordered phase boundary (which is expected to have the smallest value in this phase).

## References

- Aydin M and Yalabik M C 1989 *J. Phys. A: Math. Gen.* **22** 85  
Binder K and Stauffer D 1984 *Applications of the Monte Carlo Method in Statistical Physics (Topics in Current Physics 36)* ed K Binder (Berlin: Springer) pp 1-36  
Hornreich R M, Liebmann R, Schuster H G and Selke W 1979 *Z. Phys. B* **35** 91  
Landau D P and Binder K 1985 *Phys. Rev. B* **31** 5946  
Oitmaa J, Batchelor M T and Barber M N 1987 *J. Phys. A: Math. Gen.* **20** 1507  
Oitmaa J and Velgakis M J 1987 *J. Phys. A: Math. Gen.* **20** 1495  
Selke W 1981 *Z. Phys. B* **43** 335  
Selke W and Fisher M 1980 *Z. Phys. B* **40** 71  
Velgakis M J and Oitmaa J 1988 *J. Phys. A: Math. Gen.* **21** 547